

## Article

# Functionalization of Smart Recycled Asphalt Mixtures: A Sustainability Scientific and Pedagogical Approach

Iran Rocha Segundo <sup>1,2</sup>, Behzad Zahabizadeh <sup>3</sup>, Salmon Landi, Jr. <sup>4</sup>, Orlando Lima, Jr. <sup>1</sup>, Cátia Afonso <sup>2</sup>, Jaffer Borinelli <sup>5</sup>, Elisabete Freitas <sup>6</sup>, Vítor M. C. F. Cunha <sup>3</sup>, Vasco Teixeira <sup>2</sup>, Manuel F. M. Costa <sup>7,\*</sup> and Joaquim O. Carneiro <sup>2</sup>

<sup>1</sup> Department of Civil Engineering, University of Minho, CTAC, 4800-058 Guimarães, Portugal; iran\_gomes@hotmail.com (I.R.S.); orlandojunior.jr@hotmail.com (O.L.J.)

<sup>2</sup> Centre of Physics of Minho and Porto Universities (CF-UM-UP), Azurém Campus, University of Minho, 4800-058 Guimarães, Portugal; catiaj\_afonso@hotmail.com (C.A.); vasco@fisica.uminho.pt (V.T.); carneiro@fisica.uminho.pt (J.O.C.)

<sup>3</sup> ISISE, Institute of Science and Innovation for Bio-Sustainability (IB-S), Department of Civil Engineering, University of Minho, 4800-058 Guimarães, Portugal; b.zahabizadeh@gmail.com (B.Z.); vcunha@civil.uminho.pt (V.M.C.F.C.)

<sup>4</sup> Federal Institute Goiano, Rio Verde 75901-970, GO, Brazil; salmon.landi@ifgoiano.edu.br

<sup>5</sup> Road Engineering Research Section (RERS), EMIB, Faculty of Applied Engineering, University of Antwerp, 2020 Antwerp, Belgium; jaffer.bressanborinelli@uantwerpen.be

<sup>6</sup> ISISE, Department of Civil Engineering, University of Minho, 4800-058 Guimarães, Portugal; efreitas@civil.uminho.pt

<sup>7</sup> Centre of Physics of Minho and Porto Universities (CF-UM-UP), Gualtar Campus, University of Minho, 4710-057 Braga, Portugal

\* Correspondence: mfcosta@fisica.uminho.pt

**Citation:** Segundo, I.R.;

Zahabizadeh, B.; Landi, S., Jr.;

Lima, O., Jr.; Afonso, C.; Borinelli, J.;

Freitas, E.; Cunha, V.M.C.F.;

Teixeira, V.; Costa, M.F.M.;

et al. Functionalization of Smart

Recycled Asphalt Mixtures: A

Sustainability Scientific and

Pedagogical Approach. *Sustainability*

2022, 14, 573. <https://doi.org/10.3390/su14010573>

Academic Editor: Antonio D'Andrea

Received: 29 November 2021

Accepted: 31 December 2021

Published: 5 January 2022

**Publisher's Note:** MDPI stays neutral with regard to jurisdictional claims in published maps and institutional affiliations.



**Copyright:** © 2022 by the authors. Licensee MDPI, Basel, Switzerland. This article is an open access article distributed under the terms and conditions of the Creative Commons Attribution (CC BY) license (<https://creativecommons.org/licenses/by/4.0/>).

**Abstract:** The sustainable development of our societies demands strong efforts on scientific and technological research while informing and educating students and the general population. Air pollution and road safety hazards constitute two main public health problems that are insufficiently addressed pedagogically. With this work, we aim to contribute to tackling the problem by presenting the results of scientific research on the development of photocatalytic, superhydrophobic, and self-cleaning recycled asphalt mixtures to achieve an eco-social friendly and smart material able to mitigate socioenvironmental impacts. The functionalization of asphalt is implemented by spraying particles' solutions over a conventional AC 10, then evaluated by dye degradation and wettability. Firstly, different particles' solutions (with nano-TiO<sub>2</sub> and/or micro-PTFE under water, ethyl alcohol, and dimethyl ketone) were sprayed to select the best solution (BS), which was composed of TiO<sub>2</sub>-PTFE (4 g/L each) in ethyl alcohol. Two successive spraying coatings (diluted epoxy resin and BS) were performed over conventional and recycled AC 10 (with reclaimed asphalt pavement and steel slags). Their efficiency decreases with the highest resin amounts. The best results were obtained with 0.25 g resin and BS. For the lowest resin amount, all mixtures achieved superhydrophobicity and performed similarly regarding wettability.

**Keywords:** smart asphalt mixtures; photocatalytic asphalt mixtures; superhydrophobic asphalt mixtures; epoxy resin; functionalization process; smart coatings; sustainable road pavements

## 1. Introduction

Currently, air pollution is one of the main environmental problems, due to its effects in diverse domains, for example, the consequences for human health (pulmonary obstructions, lung cancer, cardiovascular disease (CVD), among others), the intensification of the greenhouse effect and the occurrence of acid rains. According to the World Health Organization (WHO), more than 90% of the world population lives in areas where the

concentration of pollutants exceeds the maximum limits, causing more than 4 million premature deaths, while nine out of ten breathe very polluted air [1].

Some of the main air pollutants are fine particulate matter, nitrogen oxides ( $\text{NO}_x$ ), nitric oxide (NO) and nitrogen dioxide ( $\text{NO}_2$ ), and  $\text{SO}_x$ , compounds of sulfur and oxygen molecules [2–4]. Sulfur dioxide ( $\text{SO}_2$ ) is the predominant  $\text{SO}_x$  form found in the lower atmosphere [1]. Both gases are produced in motor vehicles and also industrial processes. Recently, alternative techniques to improve urban air quality have arisen, such as capturing or reducing pollutants based on photocatalytic materials [5]. Among the photocatalysts, titanium dioxide ( $\text{TiO}_2$ ) is one of the most studied and applied semiconductors to functionalize dissimilar materials; it allows the degradation of harmful gases due to the redox photocatalytic properties when activated by UV radiation [6–8]. Nano- $\text{TiO}_2$  particles have been applied on road pavements, especially on asphalt mixtures, for air purification, due to the close proximity of the vehicles' exhaust gases [9–11].

There are several methods for functionalizing asphalt mixtures with nano- $\text{TiO}_2$ , namely volume incorporation, asphalt binder modification, spreading and spraying coating. Usually, it is applied by the spraying coating (using a painting gun) since this method requires fewer nanoparticles, which are placed just over the surface, maximizing the photocatalytic efficiency. Among the evaluation techniques available to measure the photocatalytic efficiency, the most important ones are degradation of (i) gas pollutants (for instance,  $\text{NO}_x$  and  $\text{SO}_x$ ) using a reactor and (ii) dyes (for instance, Rhodamine B, Methylene Blue, and Methylene Orange) under an aqueous solution [8].

Most of the research concerning pavements functionalization was devoted to the impact evaluation of the processes under the mechanical and rheological points of view [12–14], dope the semiconductor nanoparticles or combination with other materials to increase the photocatalytic efficiency [15,16], analyze the anti-aging effects [13,17], monitor the air quality and quantify the degradation of gases in real scale [18,19], and evaluate the  $\text{NO}_x$  depolluting performance by computational simulation [20].

These scientific works brought relevant findings considering the photocatalytic pavements. It was found that urban canyons would increase the residence time of NO, decreasing its contact with the photocatalytic surface, increasing the molecule interactions, and consequently, the photocatalytic efficiency. However, shadow areas reduce photocatalytic efficiency due to the low solar irradiation [20]. No evident  $\text{NO}_x$  degradation has been observed on a real scale since it is very difficult to evaluate on real depolluting conditions, i.e., in outdoor environments [19]. Graphitic carbon nitride (g- $\text{C}_3\text{N}_4$ )/ $\text{TiO}_2$  presented a band gap equal to 2.64 eV, while the undoped  $\text{TiO}_2$  showed 3.25 eV. Photocatalytic asphalt chip seals reached a NO photocatalytic efficiency of 31% [16].  $\text{TiO}_2$ /polystyrene-reduced graphene oxide ( $\text{TiO}_2$ /PS-rGO) retards the thermo-oxidation and UV-aging of asphalt binders [17]. The photocatalytic efficiency is lower on asphalt mixtures (functionalized by asphalt binder modification) than on cement matrix materials (functionalized by bulk incorporation) due to encapsulation of the nanoparticles by the asphalt binder. In addition, nano- $\text{TiO}_2$  increases the fatigue and aging resistances of asphalt binders [12].

To keep pavement friction on safe levels is one of the transportation engineering main concerns. The presence of water, ice, and snow over the surface drastically reduces friction contributing to the increase of road accidents [21–23]. Thus, it is essential to drain or repel the surface water quickly and remove/avoid ice and snow, which can be performed by promoting the superhydrophobic capability with the application of particles as  $\text{TiO}_2$  [24,25]  $\text{TiO}_2$  or combined with ZnO [25],  $\text{SiO}_2$  [26], PTFE [27], fluorine polymer with nano- $\text{CaO}$  [28], magnesium–aluminum layered double hydroxides [29], among others, over asphalt pavements usually by spraying coating [5,25,27–29]. A superhydrophobic surface is characterized by a high-water contact angle (higher than  $150^\circ$ ) [22,25,27].

As for the photocatalytic asphalt mixtures, the immobilization of the particles remains a challenge for the spraying coating of superhydrophobic asphalt mixtures. In addition, this capability must be evaluated in real-scale conditions to test its effectiveness

[5]. However, there is evidence that superhydrophobic coatings form an impermeable layer on the material's surface, preventing water damage [24].

Thus, besides enhancing the asphalt mixture properties, researchers are concerned with evaluating the functionalization process from different perspectives, increasing the efficiency, analysis in real scale, enhancement of immobilization process, among others. However, most studies have focused on the functionalization of a single new function. The combination of different capabilities, for instance, photocatalytic, superhydrophobic, and self-cleaning, can result in an improved final product, a multifunctional asphalt mixture. In addition, the application of these capabilities on recycled asphalt separately is rare, and together as a multifunctional material is nonexistent or unknown. However, it is strongly recommended as the eco-social friendly dimension of the civil engineering material is enhanced and the production cost reduces due to the reduction of raw materials use [5,30–33].

The main objective of the research work herein reported was to develop the photocatalytic, superhydrophobic, and self-cleaning capabilities on asphalt mixtures with improved immobilization (fixation of the particles) and analyze the functionalization process parameters. To achieve it, different solutions were set to enhance the efficiency and keep them working as long as possible by an improved immobilization process. In addition, the effect of the type of asphalt mixture (conventional or recycled with reclaimed asphalt pavement or steel slags) is analyzed. From the scientific point of view, this study contributes to the state of the art with the development of eco-social friendly pavements, extending their sustainability from the construction phase to the service life period with the possibility to photodegrade air pollutants and reduce road accidents through the superhydrophobicity capacity.

Raising awareness and educating students, as well as the general population, on environment sustainability issues, including the state-of-the art ones that we address in this paper, requires teachers and educators to have a sound scientific and technical knowledge on such advanced topics, in order to increase the effectiveness of science and technology education and the establishment of a sound scientific literacy on sustainability. From the pedagogical point of view, the study aims to contribute to raising awareness on relevant public health problems such as air pollution and road safety, to propose solutions with the dissemination of a comprehensive state of the art focusing on the development of photocatalytic, superhydrophobic, and self-cleaning capabilities on asphalt. Thus, this paper it is aimed to convey reliable information and scientific knowledge with rigorous results that educators can use with correct and up-to-date scientific data including the advances reported in this work related to the functionalization of asphalt mixtures to mitigate socioenvironmental problems.

## 2. Materials and Methods

In order to achieve the objective of this research, two steps were performed, namely: (i) the selection of the best solution sprayed over a conventional asphalt mixture and (ii) immobilization process of the particles by two successive spraying coatings (diluted epoxy resin and then the best solution, BS) over the conventional and recycled asphalt mixtures (Figure 1). In the first step, different solutions were prepared using nano-TiO<sub>2</sub> and/or micro-PTFE into water, ethyl alcohol, and dimethyl ketone mediums. Then, a conventional asphalt Mixture AC 10 was designed, compacted, cut, and subsequently sprayed with these different particle's solutions. The samples were analyzed to select the best solution (BS). In the second step, the BS was used for a successive spraying process after the spraying of a diluted resin over the conventional and recycled asphalt mixtures (composed of 30% of reclaimed asphalt pavement and 30% of steel slags both mixtures were also designed, compacted and cut before the functionalization). In both steps, the selection of the BS and immobilization process of the particles were based on the photocatalytic efficiency and water contact angle.

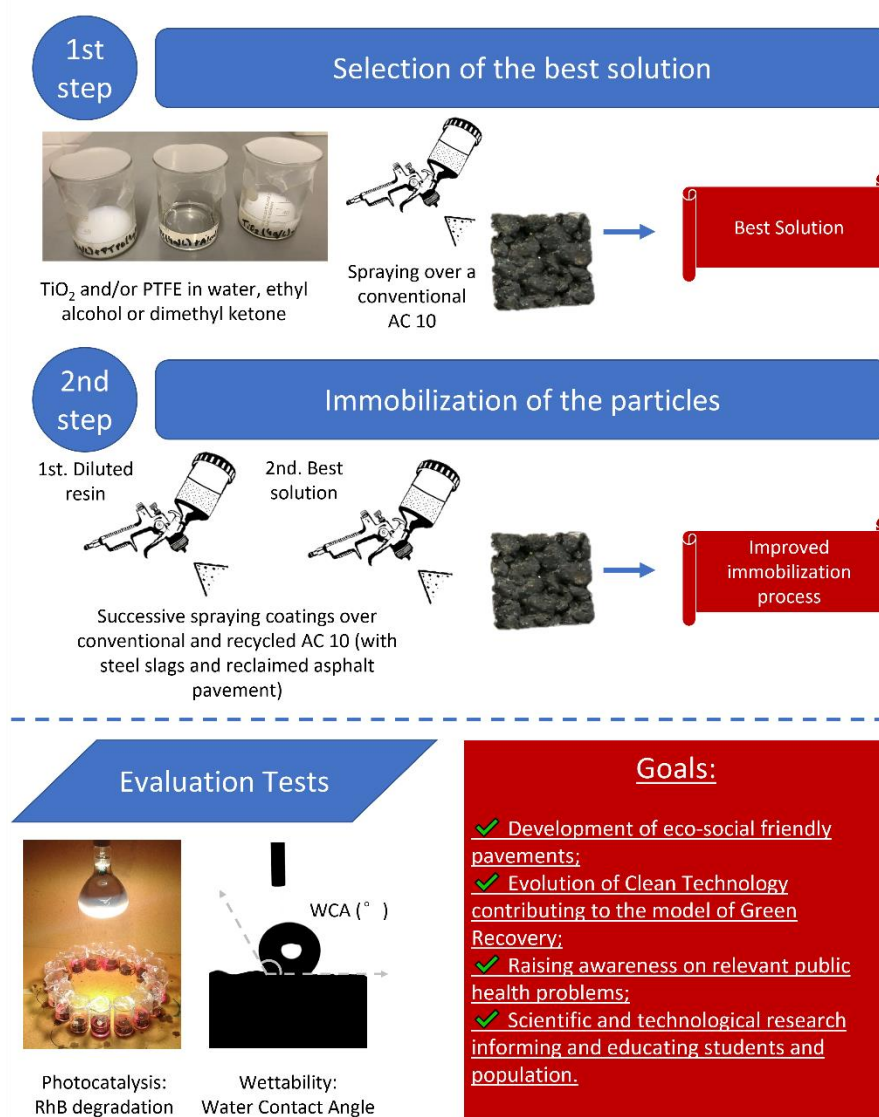


**Figure 1.** Schematic representation of the research.

### 2.1. Materials

Three AC 10 asphalt mixtures (Table 1) were adopted for this research: R—is a reference mix, F—is a mix composed of 30% reclaimed asphalt pavement (RAP), and A—is a mix composed of 30% of steel slags (SS). The use of recycled aggregates (for example SS and RAP) provides an ecological asphalt mixture from the beginning of its lifetime as presented in the section—Introduction. In this specific case, the selection of the SS for the composition of the asphalt mixture was based on the fact that iron is commonly used to dope TiO<sub>2</sub> and, therefore, increase the photocatalytic efficiency since the nature of aggregates can affect the efficiency, according to previous conclusions [34]. Furthermore, the use of SS can promote new capabilities, such as self-healing and anti-ice [5]. RAP is the most common recycled material introduced in asphalt mixtures [35]. A total of 30% of recycled material is a common content introduced to asphalt mixtures regarding the literature review and is currently applied even for the composition of road pavements.

Designed by the Marshall method, these mixtures have the same gradation and almost the same binder content, of about 5.5%. Table 1 shows their composition, asphalt binder contents (both calculated by weight), bulk density (BD), maximum bulk density (MBD), and void content (VC).

**Table 1.** Main characteristics of the asphalt mixtures.

Asphalt Mix	% 4/10	% 0/4	% Filler	% RAP 0/6	% SS 0/10	% Binder	% Virgin Binder	MBD (g/cm <sup>3</sup> )	BD (g/cm <sup>3</sup> )	VC (%)
R	68	28	4	-	-	5.5	5.5	2.428	2.305	5.1
F	67	-	3	30	-	5.4	3.5	2.446	2.334	4.6
A	42	25	3	-	30	5.4	5.5	2.676	2.569	4.0

The particles used in the functionalization process were nano-TiO<sub>2</sub> and micro-PTFE with a particle size of 1 µm. An epoxy resin with two components was selected: (i) epoxy resin composed of Bisphenol A, and (ii) cycloaliphatic polyamine adduct. According to the supplier, for pavement applications, the best mixing proportion is 2/1 in mass. Its main properties are the density of 1.10 g/cm<sup>3</sup>; ideal temperature application between 10 and 30 °C; and adhesion >3 N/mm<sup>2</sup>; curing period of 24 h. Epoxy resins are commonly used in road pavements, and they were already tested as a binder in the spreading functionalization method [27,36]. In addition, only for superhydrophobic purposes, a similar approach was carried out using a diluted epoxy resin [27].

## 2.2. Sample Preparation for the First Step (Selection of Best Solution)

First, different types of solutions were prepared with nano-TiO<sub>2</sub> and micro-PTFE with water, ethyl alcohol, and dimethyl ketone using different concentrations. It was impossible to prepare aqueous solutions with PTFE since the particles could not be dispersed into this medium. The solutions were sprayed over the cut asphalt Mixture R (reference) with 25 × 25 × 15 mm<sup>3</sup> dimensions to identify the best solution. The spraying ratio was 8 mL/cm<sup>2</sup> at room temperature. The (functionalized) asphalt mixture samples were named by an alphanumeric string, which starts by AC 10 to indicate reference asphalt concrete, the particle used (TiO<sub>2</sub> and/or PTFE), and then the solvent used (W—water, ETH—ethyl alcohol, and CET—dimethyl ketone), respectively (Table 2). When both particles, nano-TiO<sub>2</sub>, and micro-PTFE, were combined, at the end of the string, the concentration of the solution was inserted, for example, AC 10 TiO<sub>2</sub>PTFE-ETH-8g/L. In this case, 4g/L (2 g/L of nano-TiO<sub>2</sub> and 2 g/L of micro-PTFE) or 8g/L (4 g/L of nano-TiO<sub>2</sub> and 4 g/L of micro-PTFE) was included. In the case of solutions with just one type of particle, the concentration was 4 g/L. The concentrations selected were according to the literature [9,25].

**Table 2.** Mixture AC 10 (R) sprayed with different solutions.

Mixture	TiO <sub>2</sub> (g/L)	PTFE (g/L)	Solvent
AC 10	-	-	-
AC 10 TiO <sub>2</sub> -W	4	-	water
AC 10 TiO <sub>2</sub> -ETH	4	-	ethyl alcohol
AC 10 TiO <sub>2</sub> -CET	4	-	dimethyl ketone
AC 10 PTFE-ETH	-	4	ethyl alcohol
AC 10 PTFE-CET	-	4	dimethyl ketone
AC 10 TiO <sub>2</sub> PTFE-ETH-4g/L	2	2	ethyl alcohol
AC 10 TiO <sub>2</sub> PTFE-ETH-8g/L	4	4	ethyl alcohol
AC 10 TiO <sub>2</sub> PTFE-CET-4g/L	2	2	dimethyl ketone
AC 10 TiO <sub>2</sub> PTFE-CET-8g/L	4	4	dimethyl ketone

### 2.3. Sample Preparation for the Second Step (Immobilization of the Particles)

After selecting the best solution, all the (recycled and conventional) asphalt mixtures were functionalized through two successive spraying coatings: first, spraying a diluted resin epoxy and then spraying the BS, respectively (Table 3).

describes all the samples prepared in this step. The epoxy resin was diluted using butyl acetate with a proportion of 1:1 in mass.

**Table 3.** Name of the samples for the immobilization of BS.

Sample	Mixture	Diluted Resin (mg/cm <sup>2</sup> )	BS (mL/cm <sup>2</sup> )
R 0.25g	Reference	0.10	-
R 0.25g-BS			8
R 0.5g		0.20	-
R 0.5g-BS			8
R 1g		0.40	-
R 1g-BS			8
R 2g		0.80	-
R 2g-BS			8
F 0.25g	with RAP	0.10	-
F 0.25g-BS			8
F 0.5g		0.20	-
F 0.5g-BS			8
F 1g		0.40	-
F 1g-BS			8
F 2g		0.80	-
F 2g-BS			8
A 0.25g	with SS	0.10	-
A 0.25g-BS			8
A 0.5g		0.20	-
A 0.5g-BS			8
A 1g		0.40	-
A 1g-BS			8
A 2g		0.80	-
A 2g-BS			8

The cut asphalt mixtures were sprayed with 0.25, 0.50, 1, and 2 g of the diluted resin, resulting in a covering ratio of 0.1, 0.2, 0.4, and 0.8 mg/cm<sup>2</sup>. This very low covering ratio is explained by the fact that a high covering ratio could lead to the sinking of the particles. This process was similar to the one used by Arabzadeh et al. [27]. All the experiments were performed twice, and the average of the results will be presented.

### 2.4. Photocatalytic Efficiency Test

According to the literature, photocatalytic efficiency was analyzed by Rhodamine B (RhB) degradation [37,38]. The cut samples were immersed into 30 mL of 5 ppm RhB aqueous solution. The systems were arranged inside a box, 25 cm below a sunlight simulation lamp with a power intensity of 11 W/m<sup>2</sup> (acquired by a Quantum Photo Radiometer HD9021 Delta Padov). Initially, the samples were conditioned in the dark for 3 h, and then they were exposed to the light for 8 h [9,34,39]. Thus, the initial adsorption and photocatalysis were split, and this phenomenon could be analyzed precisely. To avoid the evaporation of RhB solution, which increases the solution concentration, the systems were covered with a transparent plastic film with less than 10% absorbance and reflectance (between 292 and 900 nm), allowing almost total transmittance of light to the samples.

In order to measure the photocatalytic efficiency, the maximum absorption (554 nm) of the dye was monitored as a function of the time (using a Shimadzu 3101 PC). It was calculated with Equation 1, according to [9].

$$\Phi (\%) = \left( \frac{A_0 - A}{A_0} \right) \times 100 \quad (1)$$

where  $\Phi$  is the photocatalytic efficiency,  $A$  and  $A_0$  represent the maximum absorbance of RhB (554 nm) solution for time “ $t$ ” and 0 h after irradiation, respectively.

### 2.5. Water Contact Angle Test

The samples’ water contact angle (WCA) was performed to evaluate the wettability of asphalt mixtures and characterize their hydrophilicity/hydrophobicity. The higher the WCA, the lower the wettability [5,27].

The equipment OCA 15 plus Dataphysics was used, carrying out 3 readings of 5  $\mu$ L water drop at 2 samples for 2 min, at room temperature and relative humidity (Figure 2).

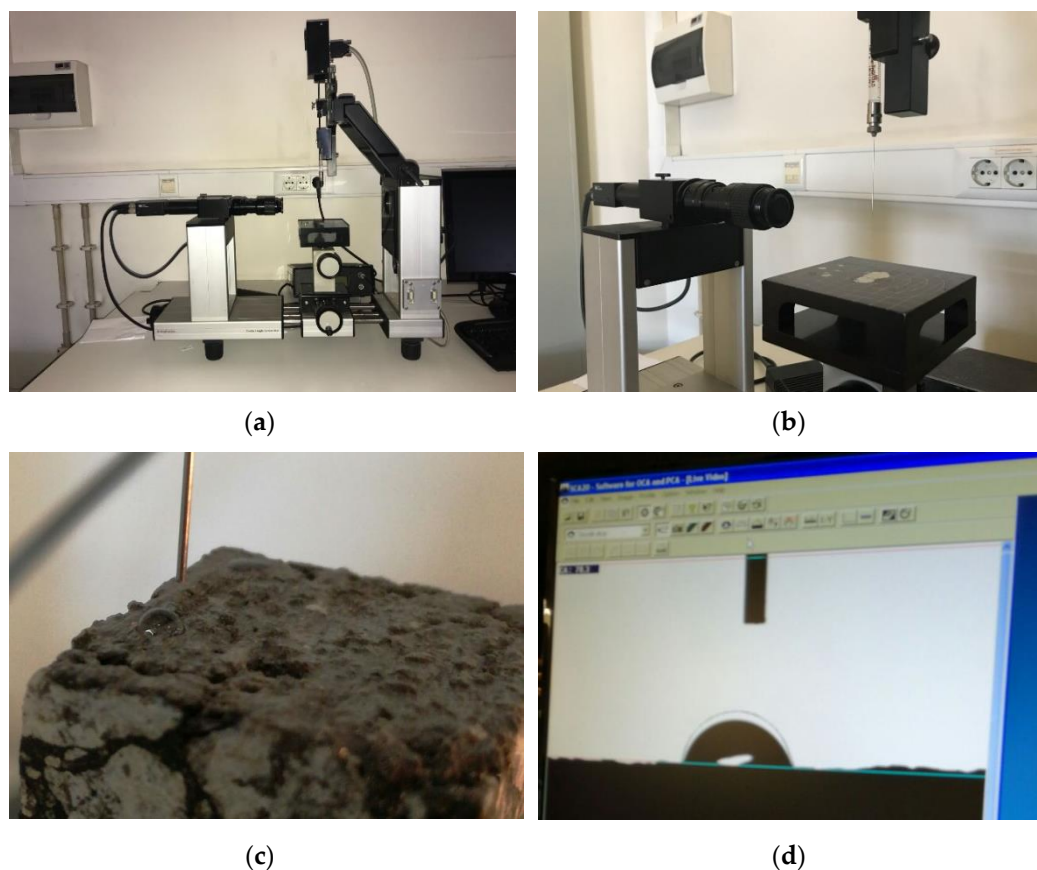


**Figure 2.** Water contact angle test: (a,b) OCA 15 plus Dataphysics; (c) detail of the water drop over the asphalt mixture samples; and (d) detail of the water drop image in the software

## 3. Results

### 3.1. Selection of Best Solution

#### 3.1.1. Photocatalytic Efficiency

The photocatalytic efficiency of all the samples tested to support selecting the best solution is presented in Figure 3. To assist the analysis, it was split according to Figure 4a particles with ketone; Figure 4b particles with ethyl alcohol; Figure 4c solvents with TiO<sub>2</sub>; Figure 4d solvents with TiO<sub>2</sub> and PTFE.

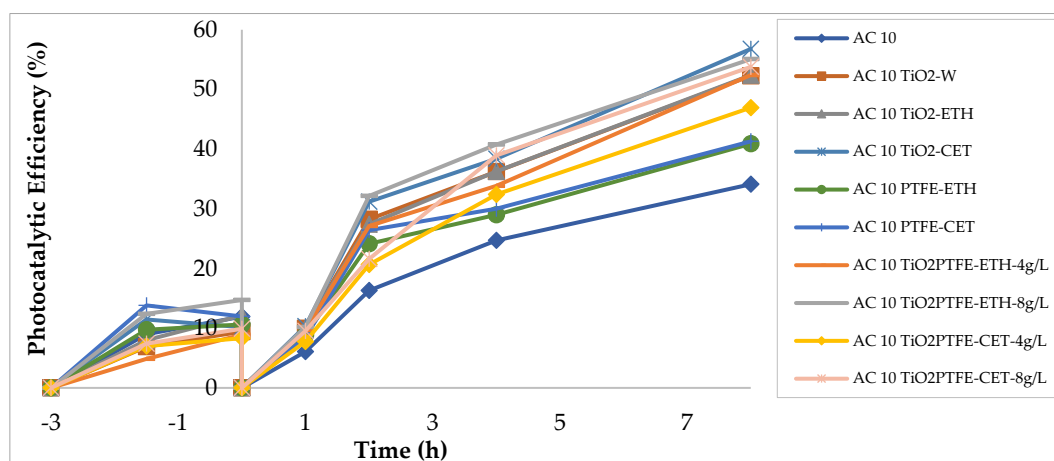
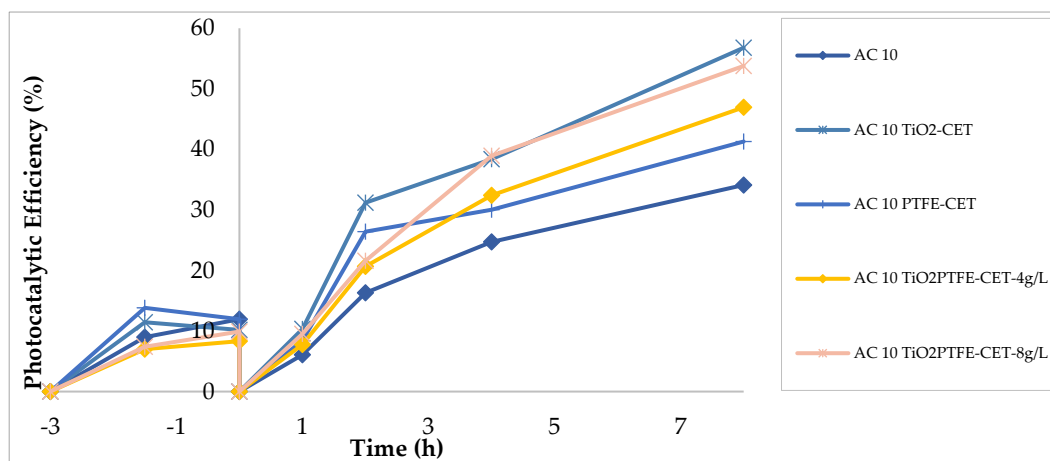
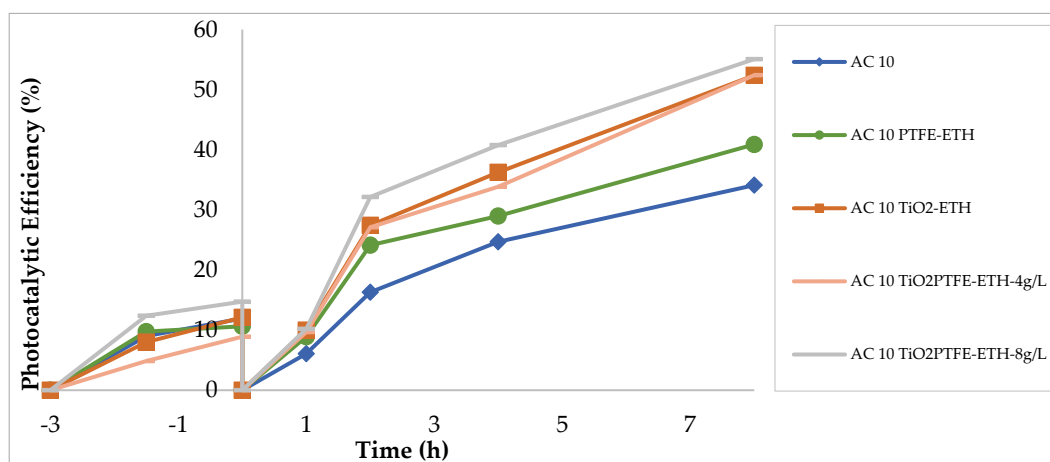


Figure 3. Photocatalytic efficiency of all the samples from the first step (selection of best solution).

A global examination of the results reveals that samples only with PTFE (AC 10 PTFE-ETH and AC 10 PTFE-CET) presented a photocatalytic efficiency 21% higher than AC 10. The samples with TiO<sub>2</sub> showed a photocatalytic efficiency at least 38% higher than the AC 10 at the end of the test, with the worst-performing results for the sample AC 10 TiO<sub>2</sub>PTFE-CET-4g/L, which increased the efficiency from 34% to 47%.

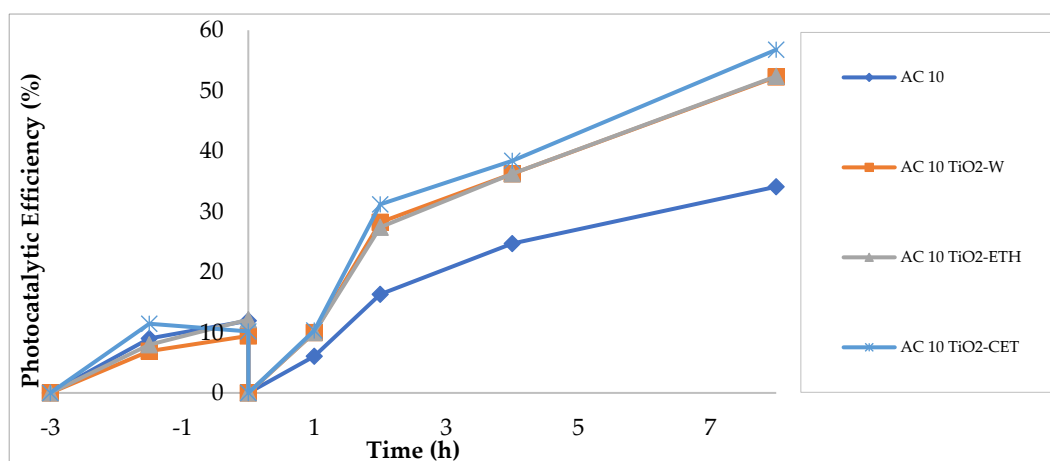


(a)

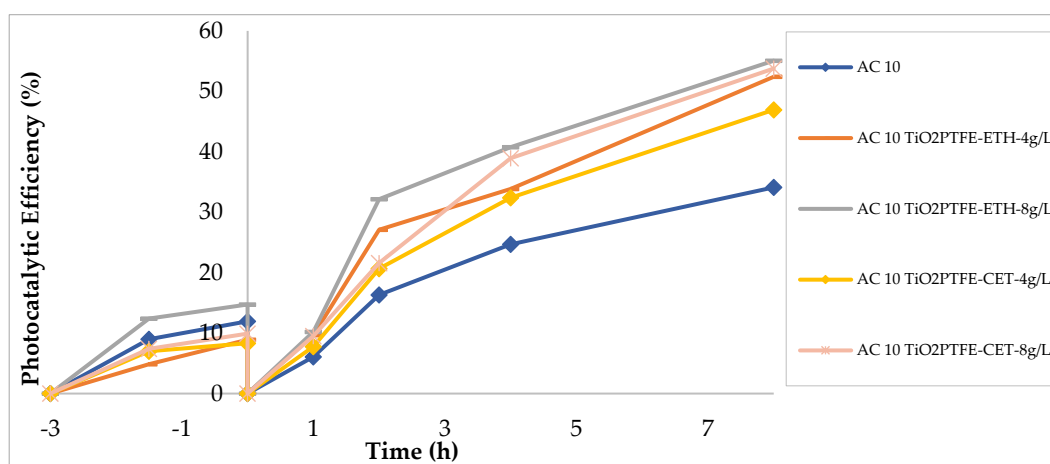


(b)





(c)



(d)

**Figure 4.** Photocatalytic efficiency of the samples comparing the: (a) particles with ketone; (b) particles with ethyl alcohol; (c) solvent with TiO<sub>2</sub>; (d) solvent with TiO<sub>2</sub> and PTFE from the first step (selection of best solution).

When ketone was used (Figure 4a), the highest efficiencies achieved were related to the use of only TiO<sub>2</sub>. When the ethyl alcohol was used (Figure 4b), the best treatment was AC 10 TiO<sub>2</sub>PTFE-ETH-8g/L, then AC 10 TiO<sub>2</sub>-ETH and AC 10 TiO<sub>2</sub>PTFE-ETH-4g/L. The effect of the solvents on the efficiency of samples with TiO<sub>2</sub> in decreasing order of performance was ketone followed by ethyl alcohol and water, with almost the same results. For the combination of the particles, the increase of the photocatalytic efficiency was 5% for the ethyl alcohol and 15% for the ketone, when the concentration increases from 4 g/L and 8 g/L. It can be seen that the best solutions achieved were TiO<sub>2</sub>-CET and TiO<sub>2</sub>-PTFE under an ethyl alcohol medium with a concentration of 8 g/L (AC 10 TiO<sub>2</sub>PTFE-ETH-8g/L).

### 3.1.2. Water Contact Angle (Wettability)

The water contact angle results are presented in Figure 5. Again, to help the analysis of the results, they were split and illustrated in Figure 6 to better compare the solvents with TiO<sub>2</sub> (Figure 6a); PTFE (Figure 6b); TiO<sub>2</sub> and PTFE (Figure 6c). Similarly, to compare the particles' performance with different mean: ketone (Figure 7a); and ethyl alcohol (Figure 7b).

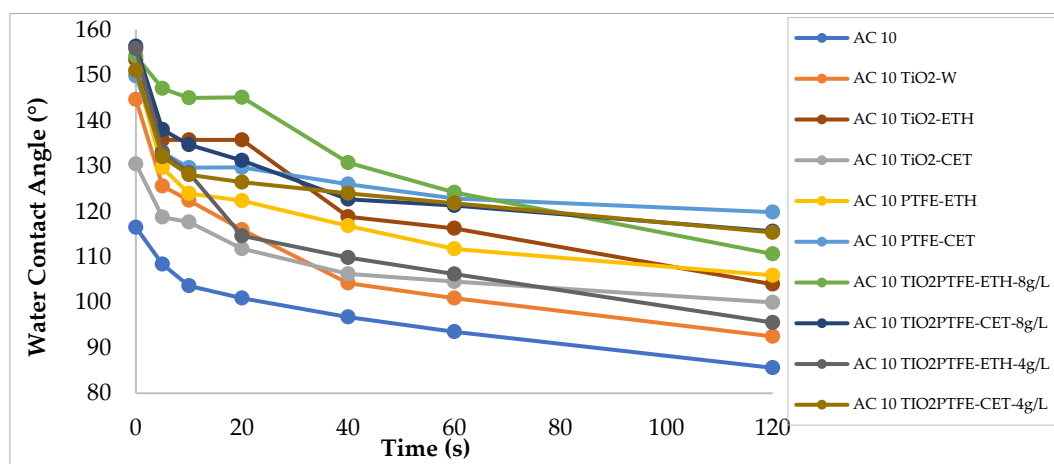
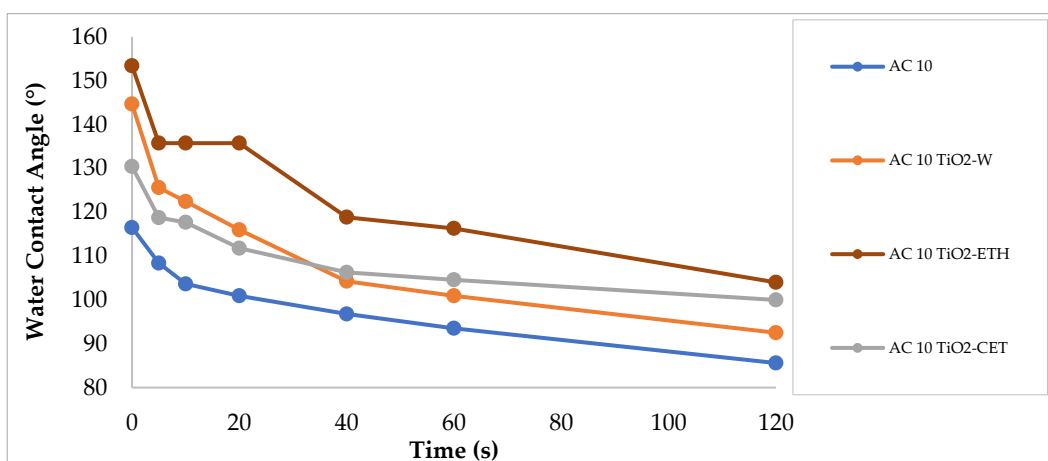
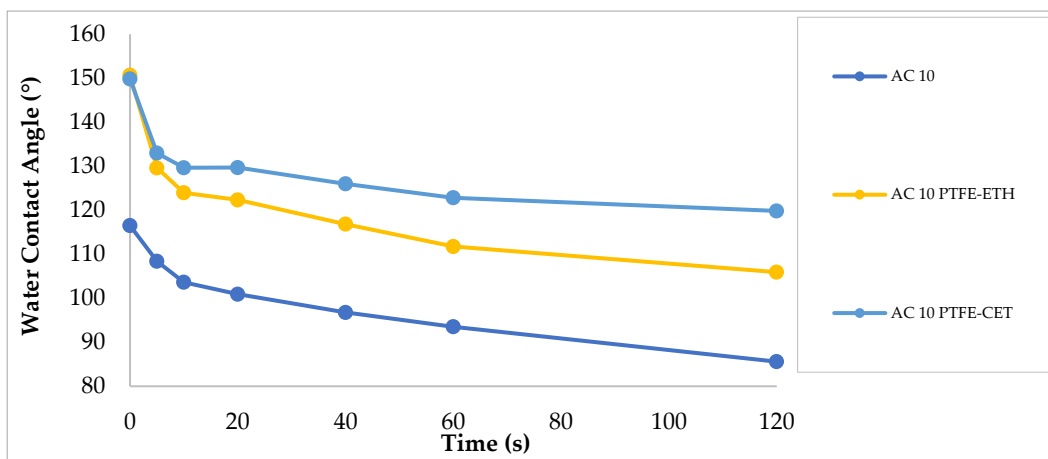


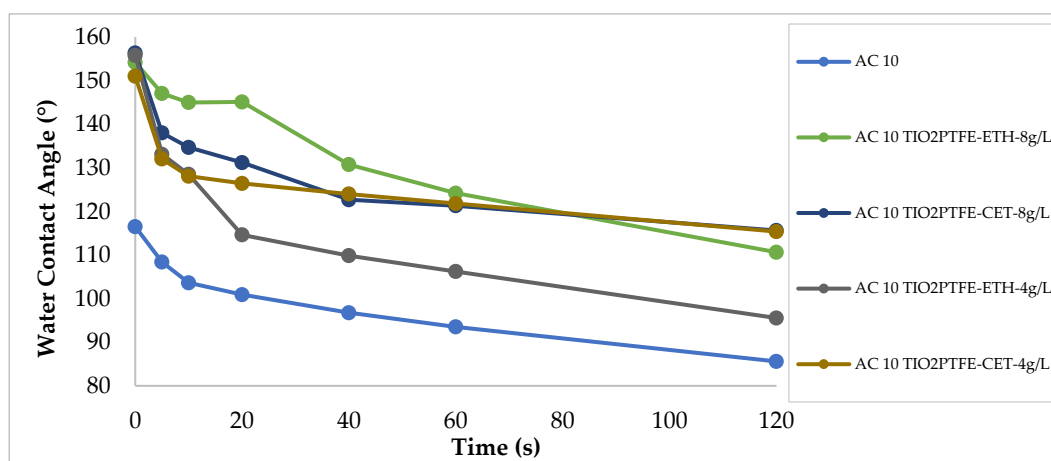
Figure 5. Results of water contact angle of all the samples from the first step (selection of best solution).



(a)



(b)



(c)

**Figure 6.** Results of water contact angle comparing the: (a) best solvent with TiO<sub>2</sub>; (b) best solvent with PTFE; (c) best solvent with TiO<sub>2</sub> and PTFE.

The reference asphalt Mixture AC 10 presented an initial WCA of 117°. All the treated samples increased the WCA when compared to AC 10. The increase was at least 11% concerning the AC 10 TiO<sub>2</sub>-CET sample. All functionalized asphalt mixtures presented a superhydrophobic capability (WCA > 150°), except those with TiO<sub>2</sub>-W (145°) and TiO<sub>2</sub>-CET (130°), which are over hydrophobic surfaces (120° < WCA < 150°). Thus, the treatments TiO<sub>2</sub>-ETH, PTFE-ETH, PTFE-CET, TiO<sub>2</sub>PTFE-ETH, and TiO<sub>2</sub>PTFE-CET provided superhydrophobic capability.

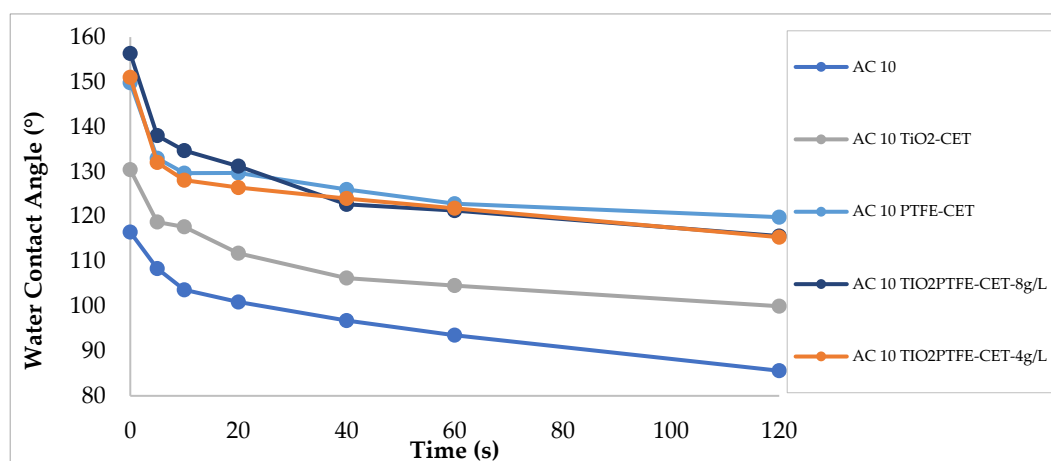
Regarding the effect of the solvents with TiO<sub>2</sub> (Figure 6a), ethyl alcohol leads to the best WCA (153°), followed by water (145°). The worst of them was with ketone (130°), as already mentioned before. For the PTFE (Figure 6b), both treatments with ketone and ethyl alcohol presented similar initial results; however, with time, the best of them was with ketone.

The increase in the concentration of TiO<sub>2</sub>-PTFE (Figures 6c and 7) was more effective for the samples with ethyl alcohol. For the whole testing, doubling the concentration leads to a WCA increase of 13% and 2% for ETH and CET samples, respectively.

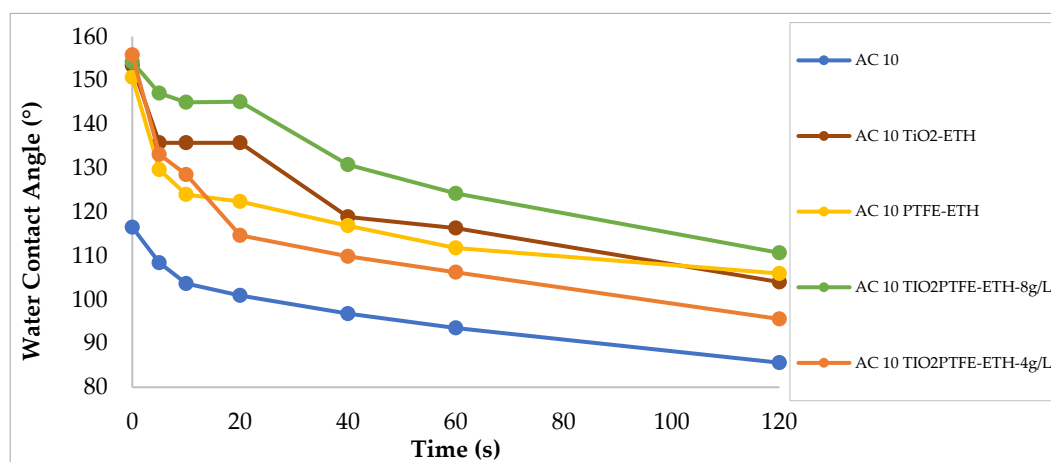
When the particles were combined, the initial WCA was similar (155°), except for AC 10 TiO<sub>2</sub>-PTFE-CET-4g/L, slightly less (151°). Nevertheless, considering the whole testing duration, it is clear that samples with higher WCA were the AC 10 TiO<sub>2</sub>PTFE-ETH-8g/L. The WCA average, from 0 to 120 s, increased 36% when compared to the reference sample. Until 20 s, this functionalized asphalt mixture showed a WCA of 145°, a much better performance than all the other samples along this testing time.

For the same solvent (Figure 7), solutions with TiO<sub>2</sub> and PTFE with a concentration of 8 g/L delivered the highest WCA. While the results for the solutions with ketone were similar, except for TiO<sub>2</sub>-CET (the worst of them), for those with ethyl alcohol, they were dispersed over time.

As the treatment designated by TiO<sub>2</sub>PTFE-ETH-8g/L was the best considering the WCA and the second one regarding photocatalysis, it was adopted as the BS to proceed with the functionalization process. The selection criteria could be based on photocatalytic efficiency. However, the treatment with the best photocatalytic efficiency (AC TiO<sub>2</sub>-CET) presented the worst WCA.



(a)



(b)

**Figure 7.** Results of water contact angle (analysis of the particles) comparing the: (a) best particles with ketone, and (b) best particles with ethyl alcohol.

### 3.2. Immobilization of BS on Recycled and Conventional Asphalt Mixtures

In this section, the photocatalytic efficiency, the water angle contact, and the effect of the asphalt mixture on wettability are addressed. For the analysis, the recycled and conventional asphalt mixtures were sprayed with two consecutive spraying coatings, specifically with the best solution (BS), TiO<sub>2</sub>PTFE-ETH-8g/L, after applying a diluted resin also by spraying.

#### 3.2.1. Photocatalytic Efficiency

Figures 8–10 show the results of the photocatalytic efficiency of the mixtures with resin and BS. In general, it can be seen that the spraying of the diluted resin decreased the photocatalytic efficiency. The samples with the highest photocatalytic efficiency are those with the least amount of resin, namely with 0.25 g and 0.5 g for all the mixtures (R-0.25g-BS and R-0.50g-BS for the Mixture R, F-0.25g-BS and F-0.25g for the Mixtures F, and A-0.25g-BS and A-0.50g for Mixture A). Nevertheless, the best performance was achieved by all mixtures characterized by 0.25g-BS.

The samples with 1 g and 2 g had the poorest photocatalytic performance. The adsorption of the pollutant (in this specific case, RhB molecules) after 3 h could help explaining the lower performance. For all the samples with resin (with or without BS), the adsorption decreased 7% on average. It represents a reduction of 3% compared to the results

without resin (see Figure 4d) and an average reduction of all results of the photocatalytic efficiency from 50% (without resin) to 28% (with resin) after 8 h of irradiation. Another explanation for the performance described could be the fact that the particles can sink into the resin. These assumptions must be further investigated.

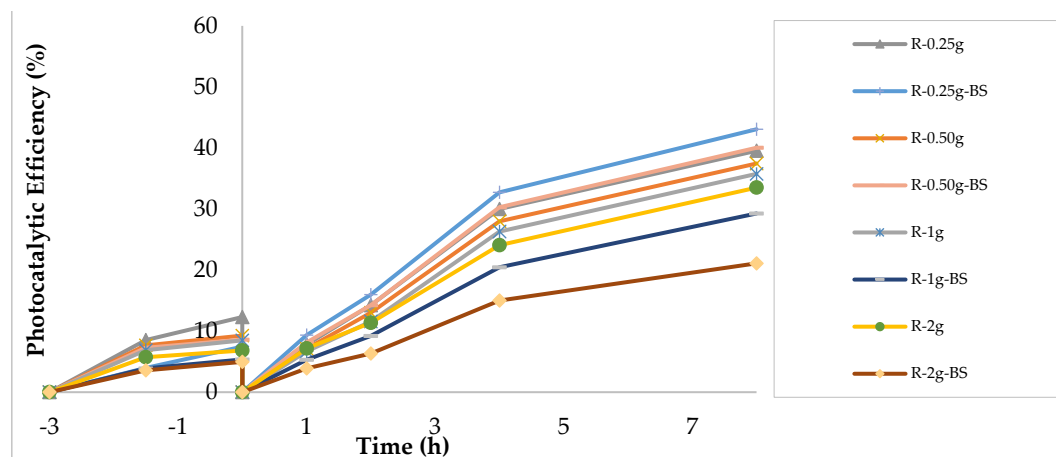


Figure 8. Results of photocatalytic efficiency of the Mixture R with resin and BS.

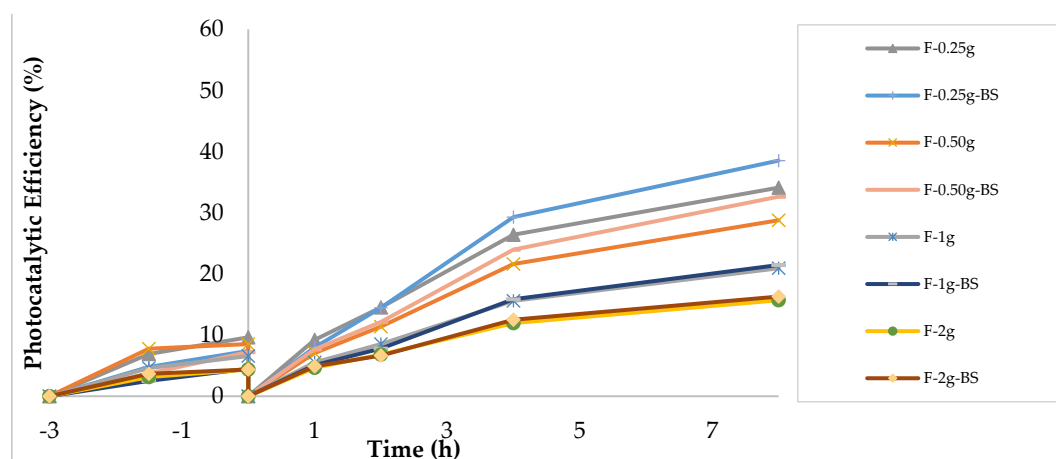


Figure 9. Results of photocatalytic efficiency of the Mixture F with resin and BS.

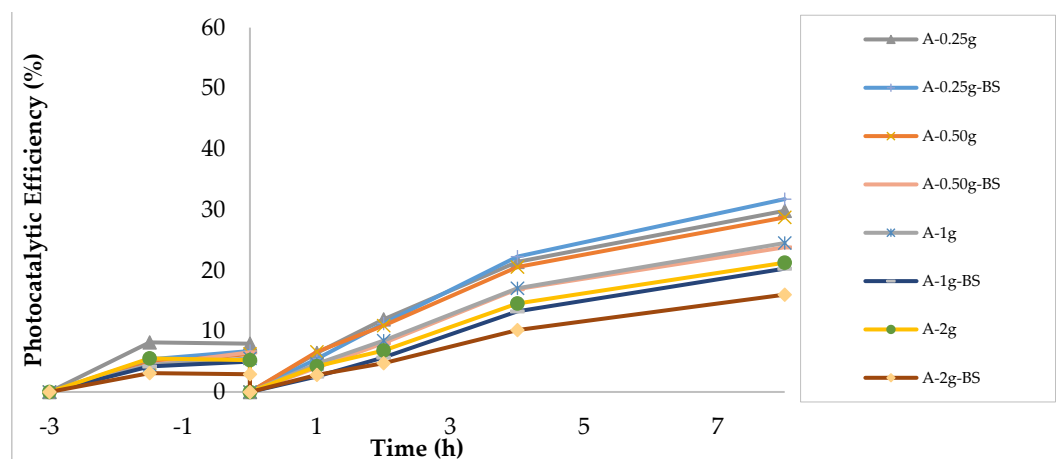
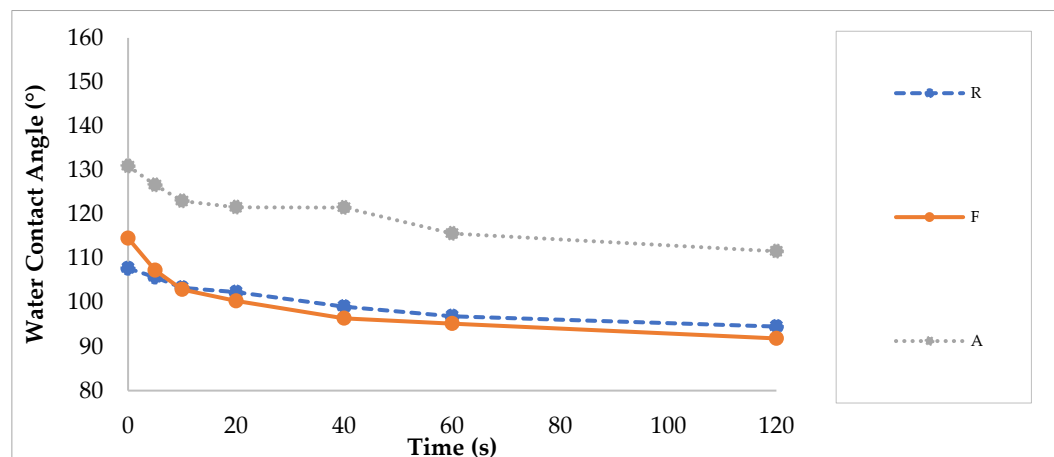


Figure 10. Results of photocatalytic efficiency of the Mixture A with resin and BS.

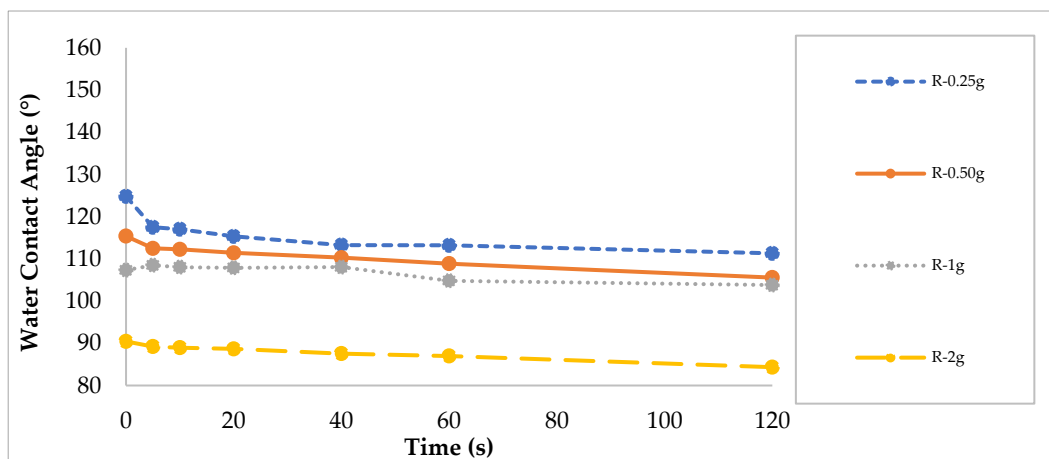
### 3.2.2. Water Contact Angle (Wettability)

Figure 11 shows the water contact angle with the time of the asphalt Mixtures R (reference), F (with 30% of RAP), and A (with 30% of SS). It can be seen that the wettability of Mixtures F and R is similar, while Mixture A is much more hydrophobic, with a WCA  $16^\circ$  superior.

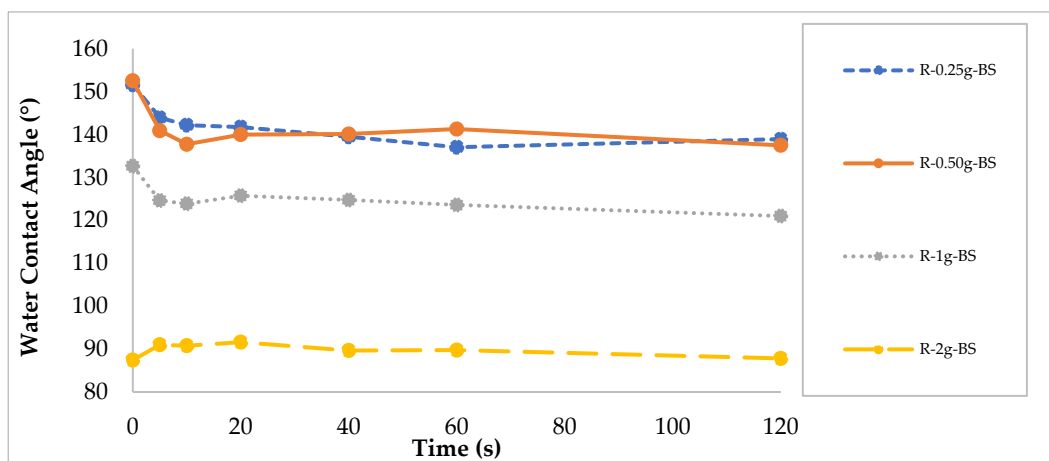


**Figure 11.** Results of water contact angle for the mixtures without treatment (R—reference, F—with 30% of RAP, and A—with 30% of SS).

Concerning Mixture R, the spraying of the resin decreases the WCA (Figure 12a). The worst WCA was achieved with 2 g, while the best one with 0.25 g. When the mixture was functionalized with BS (Figure 12b), the WCA increased for the samples with 0.25, 0.50, and 1 g of resin. Still, the superhydrophobic capability was achieved only for the first two treatments.



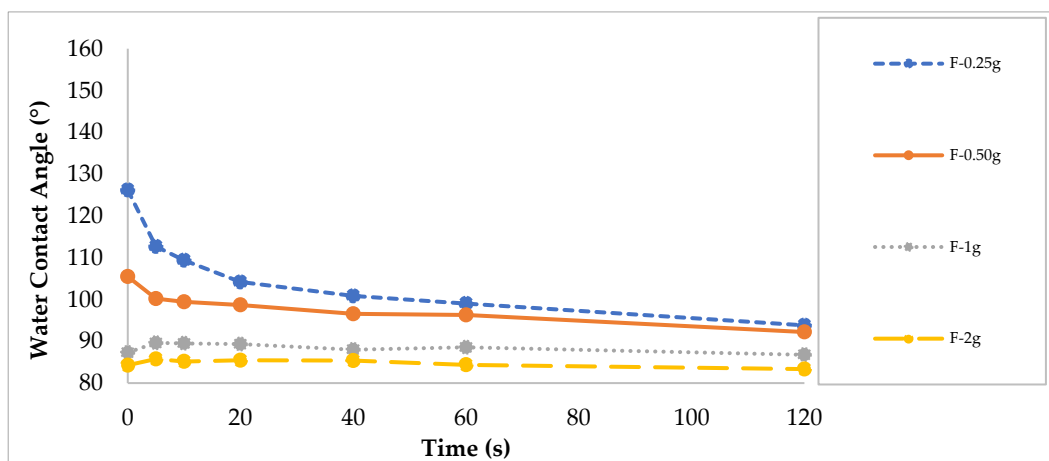
(a)



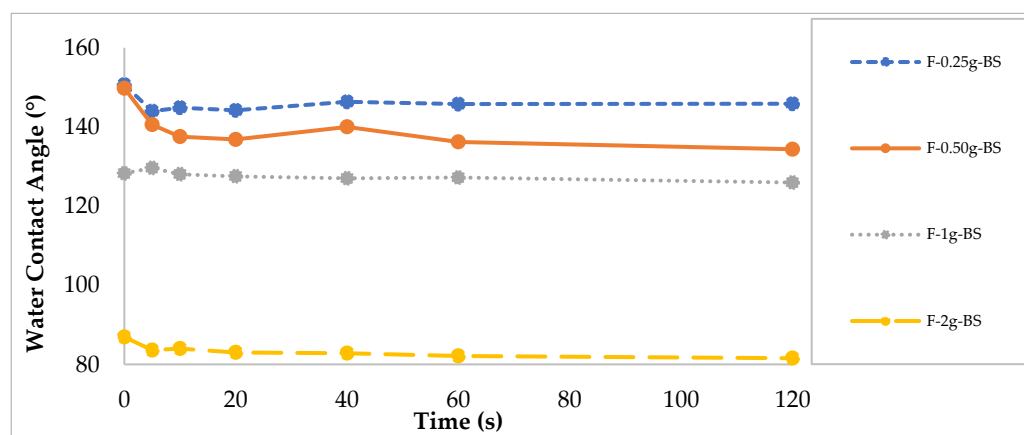
(b)

Figure 12. Results of water contact angle for Mixture R: (a) with resin, and (b) resin+BS.

In the case of Mixture F, the spraying of the resin also decreased the WCA with the resin quantity (Figure 13a). When the mixture was functionalized with BS, the WCA increased for the samples with 0.25, 0.50, and 1 g (Figure 13b). Similarly to Mixture R, the superhydrophobic capability was achieved for the samples with 0.25 and 0.50 g.



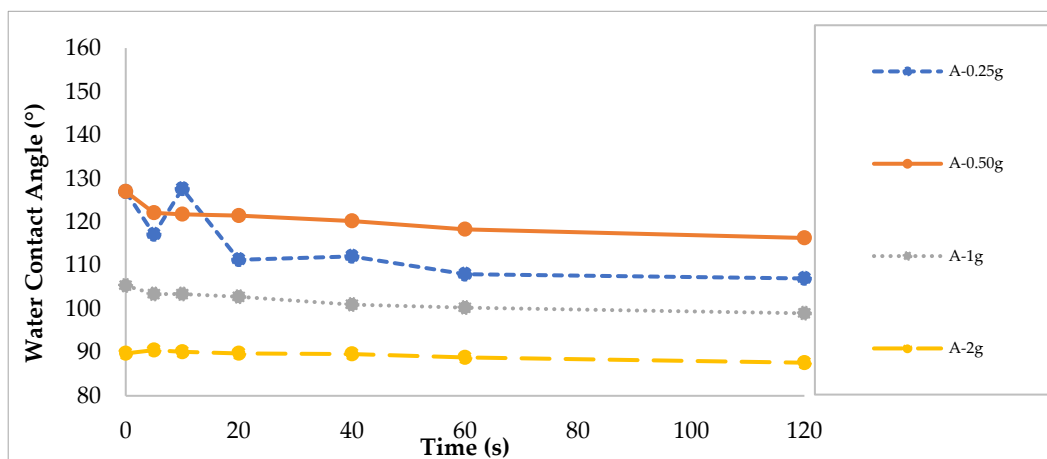
(a)



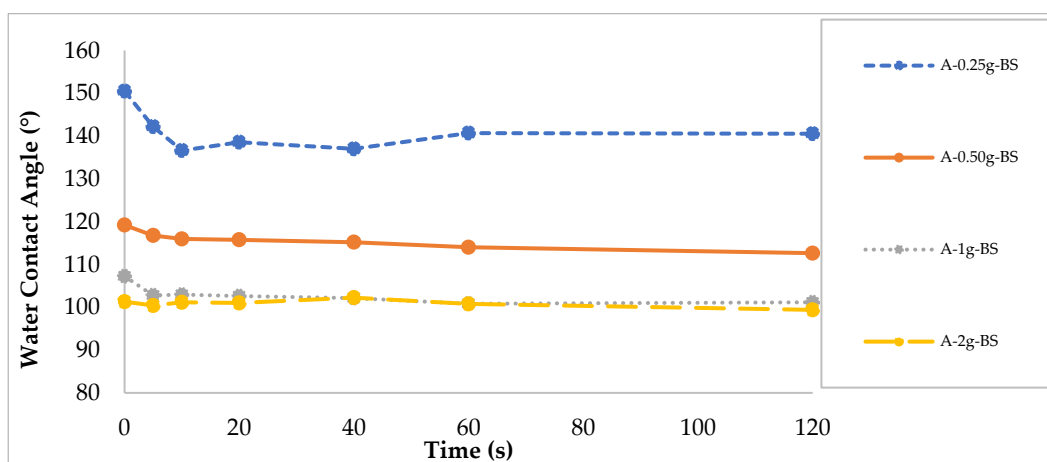
(b)

**Figure 13.** Results of water contact angle for Mixture F: (a) with resin, and (b) resin+BS.

At last, for Mixture A, the wettability results of the mixtures with resin only and with BS (Figure 14) were similar to those of Mixtures R and F, even though only the mixture treated with 0.25 g of resin developed the superhydrophobic capability.



(a)



(b)

**Figure 14.** Results of water contact angle for Mixture A: (a) with resin, and (b) resin+BS.

### 3.2.3. Effect of the Asphalt Mixture on Photocatalysis and Wettability after Functionalization Process

Regarding the effect of the asphalt mixture on the new capabilities, some topics should be addressed, namely: (i) amount of resin without and with BS on photocatalysis and wettability, (ii) photocatalytic efficiency at the end of the test and wettability during the test and at the beginning, (iii) and wettability before functionalization.

For the photocatalysis, while the reference mixture presented an average 37% of efficiency before the functionalization (with only resin for all contents), the recycled asphalt mixtures, A and F, had 26% and 25%, respectively. After the BS, the results were 33%, 27%, and 23% for R, F, and A, respectively. In conclusion, the reference mixture performed better than the recycled mixes. This performance may be explained by the composition of the aggregates, which can affect the efficiency, according to previous conclusions [34]. In addition, the adsorption (after 3 h of darkness) is higher for the reference mixture than the recycled mixtures (8% for R, 7% for F, and 6% for A on average for all results with and without BS). Higher adsorption represents a higher amount of dye over the surface of the



mixture and, consequently, over the semiconductor, degrading it more easily. These facts probably contributed to the best photocatalytic results, coming from the successive spraying coatings (0.25 g of resin and BS; 43% for R, 39% for F, and 32% for A at the end of the test). In summary, for photocatalysis, Mixture A was less effective than the other mixtures, but the conventional Mixture R presented the best photocatalytic results.

Concerning the wettability, before the application of resin and resin with BS, the asphalt mixture with SS (A) was much more hydrophobic than the other ones, without recycled materials (R) and also with RAP (F). The composition and nature of the aggregates can also explain this fact. According to previous research, SS, which compose 30% of A, is rougher than the conventional aggregates (4/10 and 0/4) and RAP [40]. In addition, their 2D form is rounder than the other aggregates [40]. These characteristics of the SS probably offered a rougher surface after the compaction for A than the other mixtures, increasing the intensity of surface energy and consequently enhancing the hydrophobicity. However, microsurface analysis, such as SEM, must be performed to confirm this hypothesis. After the successive spraying coatings, all asphalt mixtures, conventional or recycled with RAP and SS, can be used to develop a superhydrophobic surface (WCA > 150). Differently, from the expected, the asphalt mixture with F was more effective than Mixture A after the functionalization by the diluted resin and the BS. One hypothesis that can be considered is that the treatment filled the microsurface of A. However, again this fact should be better analyzed by microsurface analysis.

As presented in the section—Introduction, the use of recycled aggregate is highly recommended to provide an ecological asphalt mixture from the beginning of its lifetime. Moreover, SS have been used to introduce new capabilities to asphalt mixtures, such as self-healing and anti-ice by increasing the thermal and electrical conductivities, activated by induction or microwave heating [5,41,42]. These properties are enhanced due to the high amount of iron from the composition of the SS. In this specific research, it was also concluded that the introduction of aggregates with iron in their composition did not increase the photocatalytic efficiency, differently from expected. These new potentialities (self-healing and anti-ice) and the assessment of adverse effects will be studied in further research works.

#### 4. Conclusions

The main objective of this work was to present the process of development of photocatalytic, superhydrophobic, and self-cleaning capabilities on asphalt mixtures with improved immobilization (fixation of the particles) and to analyze the functionalization process parameters. From the scientific point of view, this study contributes to the development of eco-social friendly pavements. From the pedagogical point of view, it contributes to raising awareness on relevant public health problems such as air pollution and road safety and presenting innovative solutions to tackle them. For this, solutions composed of different solutes (particles) and solvents were used to select the best solution (BS) regarding photocatalytic efficiency and superhydrophobicity. In addition, recycled and conventional asphalt mixtures were functionalized using two consecutive spraying coatings: (i) the first one with a diluted resin and (ii) the second one with the BS. This second step aimed to improve the immobilization process of the particles over the surface of the asphalt mixtures. From the results, the following conclusions are drawn:

- For photocatalysis, the best solutions evaluated in this research were TiO<sub>2</sub>-CET and TiO<sub>2</sub>-PTFE under an ethyl alcohol medium with a concentration of 8 g/L (AC 10 TiO<sub>2</sub>PTFE-ETH-8g/L). The treatments TiO<sub>2</sub>-ETH, PTFE-ETH, PTFE-CET, TiO<sub>2</sub>PTFE-ETH, and TiO<sub>2</sub>PTFE-CET provided superhydrophobic capability.
- Concerning both capabilities, the treatment TiO<sub>2</sub>PTFE-ETH-8g/L was the best considering the WCA and the second one regarding photocatalysis; therefore it was selected as the best solution.

- The spraying of the diluted resin decreased the photocatalytic efficiency. The highest results were with 0.25g-BS for all the asphalt mixtures. The spraying of the resin reduces the WCA. The superhydrophobic capability was achieved for the samples with 0.25 and 0.50 g with BS for R and F mixtures. Mixture A achieved the superhydrophobic capability only for 0.25 g of resin.
- Recycled and conventional asphalt mixtures were functionalized with superhydrophobic capability. The asphalt mixture with reclaimed asphalt pavement was more effective than the mixture with steel slags after the functionalization by the diluted resin and the BS. For the photocatalysis, the Mixture A was also less effective than these ones. The conventional Mixture R presented the best photocatalytic results. For the lowest resin amount, all the mixtures achieved superhydrophobicity and performed similarly regarding wettability.

In general, it can be concluded that using successive spraying of a diluted resin and spraying with particles can provide the superhydrophobic capability for low amounts of resin (less than 0.50 g). The photocatalytic capability decreased with the use of the resin. The highest the use of resin, the lowest the photocatalytic efficiency. The best results were for 0.25 g of resin with BS. However, more studies are essential to explain the results and consequently to improve them. One hypothesis is that the particles can sink in the thick layers of resin losing their effectiveness for the new capabilities.

Multifunctional and smart recycled asphalt mixtures can be included in the domain of clean technology and, in this circumstance, contribute to the transition to a new sustainable model “Green Recovery”. In addition, this work showed that the civil engineering field is an important potential destination for applying nanomaterials on a large scale, which can promote the dynamism of the nanomaterial industry. Further, the introduction of recycled materials in asphalt mixtures is strongly recommended since their incorporation increases the sustainability of road pavements from the beginning of the lifetime even before the service life period. This work also showed that this theme analyzed under a sustainability perspective is relevant in pedagogical terms, once it brings great contributions to human health and road safety and should be included in the education of our youngsters and in life-long learning because the society and the environment need actions to mitigate the problems related to road accidents and air pollution.

The next steps of this research from the scientific point of view will be: (i) microsurface analysis in order to confirm the hypothesis that the nano/microparticles sink into the resin layer; (ii) gas degradation (namely  $\text{NO}_x$  and  $\text{SO}_2$ ) in order to evaluate the photocatalytic efficiency of the functionalized asphalt mixtures under the air purification perspective; (iii) assessment of the friction under different conditions (namely, iced, wet and dry) to confirm the contribution of the particles to the mitigation of road safety problems; (iv) submission of wearing (abrasion) in the functionalized asphalt mixtures in order to verify the particles’ immobilization; and (v) evaluation of new potentialities of the use of steel slags (SS) (namely, self-healing and anti-ice) and the assessment of its adverse effects.

**Author Contributions:** Conceptualization, I.R.S., E.F. and J.O.C.; methodology, I.R.S., E.F., J.O.C.; validation, B.Z., J.B., E.F., S.L.J.; formal analysis, B.Z., J.B., I.R.S. and S.L.J.; investigation, I.R.S., E.F., and J.O.C.; resources, E.F., M.F.M.C., V.T. and J.O.C.; data curation, S.L.J.; writing—original draft preparation, I.R.S., O.L.J., C.A.; writing—review and editing, E.F., M.F.M.C., V.M.C.F.C., V.T. and J.O.C.; visualization, E.F., M.F.M.C., J.O.C., I.R.S.; supervision, E.F. and J.O.C.; project administration, J.O.C.; funding acquisition, E.F., M.F.M.C., V.T. and J.O.C. All authors have read and agreed to the published version of the manuscript.

**Funding:** This research was funded by the Portuguese Foundation for Science and Technology (FCT), PhD scholarships SFRH/BD/137421/2018 and SFRH/BD/143636/2019, NanoAir PTDC/FIS-MAC/6606/2020, UIDB/04650/2020, and UIDB/04029/2020.

**Institutional Review Board Statement:** Not applicable.

**Informed Consent Statement:** Not applicable.

**Data Availability Statement:** Not applicable.

**Conflicts of Interest:** The authors declare no conflicts of interest.

## References

1. World Health Organization. *WHO Global Air Quality Guidelines. Particulate Matter (PM<sub>2.5</sub> and PM<sub>10</sub>), Ozone, Nitrogen Dioxide, Sulfur Dioxide and Carbon Monoxide*; World Health Organization: Geneva, Switzerland, 2021; ISBN 978-92-4-003422-8.
2. Giunta, M.; Lo Bosco, D.; Leonardi, G.; Scopelliti, F. Estimation of Gas and Dust Emissions in Construction Sites of a Motorway Project. *Sustainability* **2019**, *11*, 7218. <https://doi.org/10.3390/su11247218>.
3. Giunta, M. Assessment of the Impact of CO, NO<sub>x</sub> and PM<sub>10</sub> on Air Quality during Road Construction and Operation Phases. *Sustainability* **2020**, *12*, 10549. <https://doi.org/10.3390/su122410549>.
4. Giunta, M. Assessment of the environmental impact of road construction: Modelling and prediction of fine particulate matter emissions. *Build. Environ.* **2020**, *176*, 106865. <https://doi.org/10.1016/j.buildenv.2020.106865>.
5. Segundo, I.R.; Freitas, E.; Branco, V.T.F.C.; Landi, S.; Costa, M.F.; Carneiro, J.O. Review and analysis of advances in functionalized, smart, and multifunctional asphalt mixtures. *Renew. Sustain. Energy Rev.* **2021**, *151*, 111552. <https://doi.org/10.1016/j.rser.2021.111552>.
6. Zabihi-Mobarakeh, H.; Nezamzadeh-Ejhi, A. Application of supported TiO<sub>2</sub> onto Iranian clinoptilolite nanoparticles in the photodegradation of mixture of aniline and 2, 4-dinitroaniline aqueous solution. *J. Ind. Eng. Chem.* **2015**, *26*, 315–321. <https://doi.org/10.1016/j.jiec.2014.12.003>.
7. Nezamzadeh-Ejhi, A.; Bahrami, M. Investigation of the photocatalytic activity of supported ZnO–TiO<sub>2</sub> on clinoptilolite nanoparticles towards photodegradation of wastewater-contained phenol. *Desalin. Water Treat.* **2015**, *55*, 1096–1104. <https://doi.org/10.1080/19443994.2014.922443>.
8. Rocha Segundo, I.; Freitas, E.; Landi Jr, S.; Costa, M.F.M.; Carneiro, J.O. Smart, Photocatalytic and Self-Cleaning Asphalt Mixtures: A Literature Review. *Coatings* **2019**, *9*, 696. <https://doi.org/10.3390/coatings9110696>.
9. Carneiro, J.O.O.; Azevedo, S.; Teixeira, V.; Fernandes, F.; Freitas, E.; Silva, H.; Oliveira, J. Development of photocatalytic asphalt mixtures by the deposition and volumetric incorporation of TiO<sub>2</sub> nanoparticles. *Constr. Build. Mater.* **2013**, *38*, 594–601. <https://doi.org/10.1016/j.conbuildmat.2012.09.005>.
10. Yu, H.; Dai, W.; Qian, G.; Gong, X.; Zhou, D.; Li, X.; Zhou, X. The NO<sub>x</sub> degradation performance of nano-TiO<sub>2</sub> coating for asphalt pavement. *Nanomaterials* **2020**, *10*, 897. <https://doi.org/10.3390/nano10050897>.
11. Bocci, E.; Riderelli, L.; Fava, G.; Bocci, M. Durability of NO Oxidation Effectiveness of Pavement Surfaces Treated with Photocatalytic Titanium Dioxide. *Arab. J. Sci. Eng.* **2016**, *1*–7. <https://doi.org/10.1007/s13369-016-2168-5>.
12. Dell’Antonio Cadorin, N.; Victor Staub de Melo, J.; Borba Broering, W.; Luiz Manfro, A.; Salgado Barra, B. Asphalt nanocomposite with titanium dioxide: Mechanical, rheological and photoactivity performance. *Constr. Build. Mater.* **2021**, *289*, 18–25. <https://doi.org/10.1016/j.conbuildmat.2021.123178>.
13. Trujillo-Valladolid, M.; Alcántar-Vázquez, B.; Ramírez-Zamora, R.M.; Ossa-López, A. Influence of aging on the physicochemical behavior of photocatalytic asphalt cements subjected to the natural environment. *Constr. Build. Mater.* **2021**, *295*, 123597. <https://doi.org/10.1016/j.conbuildmat.2021.123597>.
14. Fakhri, M.; shahryari, E. The effects of nano zinc oxide (ZnO) and nano reduced graphene oxide (RGO) on moisture susceptibility property of stone mastic asphalt (SMA). *Case Stud. Constr. Mater.* **2021**, *15*, e00655. <https://doi.org/10.1016/j.cscm.2021.e00655>.
15. Chen, C.; Tang, B.; Cao, X.; Gu, F.; Huang, W. Enhanced photocatalytic decomposition of NO on portland cement concrete pavement using nano-TiO<sub>2</sub> suspension. *Constr. Build. Mater.* **2021**, *275*, 122135. <https://doi.org/10.1016/j.conbuildmat.2020.122135>.
16. Cao, X.; Deng, M.; Tang, B.; Ding, Y.; Yang, X. Development of photocatalytic chip seal for nitric oxide removal on the surface of pavement using g-C<sub>3</sub>N<sub>4</sub>/TiO<sub>2</sub> composite. *Road Mater. Pavement Des.* **2021**, *22*, 1178–1194. <https://doi.org/10.1080/14680629.2019.1687008>.
17. Yang, J.; Muhammad, Y.; Yang, C.; Liu, Y.; Su, Z.; Wei, Y.; Li, J. Preparation of TiO<sub>2</sub>/PS-rGO incorporated SBS modified asphalt with enhanced resistance against ultraviolet aging. *Constr. Build. Mater.* **2021**, *276*, 121461. <https://doi.org/10.1016/j.conbuildmat.2020.121461>.
18. Jensen, H.; Pedersen, P.D. Real-life Field Studies of the NO<sub>x</sub> Removing Properties of Photocatalytic Surfaces in Roskilde and Copenhagen Airport, Denmark. *J. Photocatal.* **2020**, *2*, 71–81. <https://doi.org/10.2174/2665976x01999200811155905>.
19. Fernández-Pampillón, J.; Palacios, M.; Núñez, L.; Pujadas, M.; Sanchez, B.; Santiago, J.L.; Martilli, A. NO<sub>x</sub> depolluting performance of photocatalytic materials in an urban area—Part I: Monitoring ambient impact. *Atmos. Environ.* **2021**, *251*. <https://doi.org/10.1016/j.atmosenv.2021.118190>.
20. Sanchez, B.; Santiago, J.L.; Martilli, A.; Palacios, M.; Núñez, L.; Pujadas, M.; Fernández-Pampillón, J. NO<sub>x</sub> depolluting performance of photocatalytic materials in an urban area—Part II: Assessment through Computational Fluid Dynamics simulations. *Atmos. Environ.* **2021**, *246*. <https://doi.org/10.1016/j.atmosenv.2020.118091>.
21. Dalhat, M.A. Water resistance and characteristics of asphalt surfaces treated with micronized-recycled-polypropylene waste: Super-hydrophobicity. *Constr. Build. Mater.* **2021**, *285*, 122870. <https://doi.org/10.1016/j.conbuildmat.2021.122870>.

22. Lee, E.; Kim, D.H. Simple fabrication of asphalt-based superhydrophobic surface with controllable wetting transition from Cassie-Baxter to Wenzel wetting state. *Colloids Surfaces A Physicochem. Eng. Asp.* **2021**, *625*, 126927. <https://doi.org/10.1016/j.colsurfa.2021.126927>.
23. Baheri, F.T.; Poulidakos, L.D.; Poulidakos, D.; Schutzius, T.M. Ice adhesion behavior of heterogeneous bituminous surfaces. *Cold Reg. Sci. Technol.* **2021**, *192*, 103405. <https://doi.org/10.1016/j.coldregions.2021.103405>.
24. Wu, C.; Li, L.; Wang, W.; Gu, Z.; Li, H.; Lin, X.; Wang, H. Coating on Asphalt Pavement. *Nanomaterials* **2021**, *11*, 1–19.
25. Rocha Segundo, I.; Ferreira, C.; Freitas, E.F.; Carneiro, J.O.; Fernandes, F.; Júnior, S.L.; Costa, M.F.; Landi Júnior, S.; Costa, M.F. Assessment of photocatalytic, superhydrophobic and self-cleaning properties on hot mix asphalts coated with TiO<sub>2</sub> and/or ZnO aqueous solutions. *Constr. Build. Mater.* **2018**, *166*, 36–44. <https://doi.org/10.1016/j.conbuildmat.2018.01.106>.
26. Gao, Y.; Qu, L.; He, B.; Dai, K.; Fang, Z.; Zhu, R. Study on effectiveness of anti-icing and deicing performance of superhydrophobic asphalt concrete. *Constr. Build. Mater.* **2018**, *191*, 270–280. <https://doi.org/10.1016/j.conbuildmat.2018.10.009>.
27. Arabzadeh, A.; Ceylan, H.; Kim, S.; Gopalakrishnan, K.; Sassani, A. Superhydrophobic Coatings on Asphalt Concrete Surfaces. *Transp. Res. Rec. J. Transp. Res. Board* **2016**, *2551*, 10–17. <https://doi.org/10.3141/2551-02>.
28. Nascimento, J.H.O.; Pereira, P.; Freitas, E.; Fernandes, F. Development and characterization of a superhydrophobic and anti-ice asphaltic nanostructured material for road pavements. In Proceedings of the 7th International Conference on Maintenance and Rehabilitation of Pavements and Technological Control, At Auckland, New Zealand, 28–30 August 2012.
29. Peng, C.; Zhang, H.; You, Z.; Xu, F.; Jiang, G.; Lv, S.; Zhang, R. Preparation and anti-icing properties of a superhydrophobic silicone coating on asphalt mixture. *Constr. Build. Mater.* **2018**, *189*, 227–235. <https://doi.org/10.1016/j.conbuildmat.2018.08.211>.
30. Torres de Rosso, L.; Victor Staub de Melo, J. Impact of incorporating recycled glass on the photocatalytic capacity of paving concrete blocks. *Constr. Build. Mater.* **2020**, *259*, 119778. <https://doi.org/10.1016/j.conbuildmat.2020.119778>.
31. Xu, Y.; Chen, W.; Jin, R.; Shen, J.; Smallbone, K.; Yan, C.; Hu, L. Experimental investigation of photocatalytic effects of concrete in air purification adopting entire concrete waste reuse model. *J. Hazard. Mater.* **2018**, *353*, 421–430. <https://doi.org/10.1016/j.jhazmat.2018.04.030>.
32. Praticò, F.G.; Vaiana, R.; Giunta, M. Sustainable Rehabilitation of Porous European Mixes. In *Proceedings of the ICSDC 2011*; American Society of Civil Engineers: Reston, VA, USA, 2012; pp. 535–541.
33. Praticò, F.G.; Giunta, M.; Mistretta, M.; Gulotta, T.M. Energy and Environmental Life Cycle Assessment of Sustainable Pavement Materials and Technologies for Urban Roads. *Sustainability* **2020**, *12*, 704. <https://doi.org/10.3390/su12020704>.
34. Rocha Segundo, I.; Landi Jr., S.; Oliveira, S.M.B.; Freitas, E.F. de; Carneiro, J.A.O. Photocatalytic Asphalt Mixtures: Mechanical Performance and Impacts of Traffic and Weathering Abrasion on Photocatalytic Efficiency. *Catal. Today* **2018**. <https://doi.org/10.1016/j.cattod.2018.07.012>.
35. Akhtar Hossain, M. Effect of Water Submergence on the Characteristics of Bituminous Mixes Using Reclaimed Asphalt Pavement. *Eur. J. Biophys.* **2018**, *6*, 1. <https://doi.org/10.11648/j.ejb.20180601.11>.
36. Wang, D.; Leng, Z.; Hüben, M.; Oeser, M.; Steinauer, B. Photocatalytic pavements with epoxy-bonded TiO<sub>2</sub>-containing spreading material. *Constr. Build. Mater.* **2016**, *107*, 44–51. <https://doi.org/10.1016/j.conbuildmat.2015.12.164>.
37. Zhang, W.; Xiao, X.; Zeng, X.; Li, Y.; Zheng, L.; Wan, C. Enhanced photocatalytic activity of TiO<sub>2</sub> nanoparticles using SnS<sub>2</sub>/RGO hybrid as co-catalyst: DFT study and photocatalytic mechanism. *J. Alloys Compd.* **2016**, *685*, 774–783. <https://doi.org/10.1016/j.jallcom.2016.06.199>.
38. Madhukar, B.; Wiener, J.; Militky, J.; Rwwaïre, S.; Mishra, R.; Jacob, K.I.; Wang, Y.; Kale, B.M.; Wiener, J.; Militky, J.; et al. Coating of cellulose-TiO<sub>2</sub> nanoparticles on cotton fabric for durable photocatalytic self-cleaning and stiffness. *Carbohydr. Polym.* **2016**, *150*, 107–113. <https://doi.org/10.1016/j.carbpol.2016.05.006>.
39. Zahabizadeh, B.; Segundo, I.R.; Pereira, J.; Freitas, E.; Camões, A.; Tavares, C.J.; Teixeira, V.; Cunha, V.M.C.F.; Costa, M.F.M.; Carneiro, J.O. Development of Photocatalytic 3D-Printed Cementitious Mortars: Influence of the Curing, Spraying Time Gaps and TiO<sub>2</sub> Coating Rates. *Buildings* **2021**, *11*, 381. <https://doi.org/10.3390/buildings11090381>.
40. Rocha Segundo, I.; Freitas, E.; Costa, M.F.; Carneiro, J. Incorporation of steel slag and reclaimed asphalt into pavement surface layers. In Proceedings of the 5th International Conference WASTES: Solutions, Treatments and Opportunities, Lisbon, Portugal, 4–6 September 2019.
41. Gao, J.; Sha, A.; Wang, Z.; Tong, Z.; Liu, Z. Utilization of steel slag as aggregate in asphalt mixtures for microwave deicing. *J. Clean. Prod.* **2017**, *152*, 429–442. <https://doi.org/10.1016/j.jclepro.2017.03.113>.
42. Sun, Y.; Liu, Q.; Wu, S.; Shang, F. Microwave heating of steel slag asphalt mixture. *Key Eng. Mater.* **2014**, *599*, 193–197. <https://doi.org/10.4028/www.scientific.net/KEM.599.193>.